# Relative RADAR Cross Section based Feature Identification with Millimetre Wave RADAR for Outdoor SLAM

Ebi Jose
School of Electrical and Electronic Engineering
Nanyang Technological University
Nanyang Avenue 639798, Singapore.
Email:ebi@pmail.ntu.edu.sg

Martin D. Adams
School of Electrical and Electronic Engineering
Nanyang Technological University
Nanyang Avenue 639798, Singapore.
Email: eadams@ntu.edu.sg

*Abstract*— **Millimetre Wave RADARs are more robust than most other sensors used in outdoor autonomous navigation in that their performance is less affected by dust, fog, moderate rain or snow and ambient lighting conditions. Millimetre Wave (MMW) RADAR differs from other range sensors as it can provide complete power returns for many points down range. In addition, MMW RADAR has a comparatively long range which can enable a vehicle to localise efficiently when there are only a few features in the environment.**

**A method for estimating the relative RADAR cross section of objects is explained. This is useful in SLAM as we can predict the relative RCS of objects based on predicted observations which will allow feature discrimination so that features can be identified by parameters other than their coordinates. A new augmented state vector for an Extended Kalman Filter is introduced which includes the relative RADAR cross sections of features, and the RADAR constants and losses along with the usual vehicle pose and feature locations. An estimate of the received noise when a target is present and in target absence has been carried out for accurately predicting the RADAR power-range spectra. Finally a SLAM formulation using the proposed methods is shown. This work is a step towards robust outdoor SLAM with MMW RADAR based continuous power spectra.**

## I. Introduction

MMW RADAR provides consistent and fairly accurate range measurements for the environmental imaging required to perform SLAM in dusty, foggy and poorly illuminated environments. Millimetre wave RADAR signals have the ability to penetrate many objects and can provide information for distributed targets that appear in a single observation. This work is conducted with a 77 GHz Frequency Modulated Continuous Wave (FMCW) RADAR which operates in the millimetre wave region of the Electro-Magnetic Spectrum.

For SLAM, it is necessary to predict the target locations accurately given a prediction of the vehicle/RADAR location. A method for accurately predicting the power-range spectra (or range bins) using the RADAR range equation and the knowledge of the noise distributions in the RADAR is initially explained in this paper.

A mobile robot SLAM problem is then formulated which estimates, robot pose, 2D target positions, target relative RADAR cross sections (RCSs) and certain RADAR parameters which include transmitted RADAR signal power losses. Predicted observations are formed using this predicted state and the RADAR equation, and a noise analysis to construct "predicted range-bins". The actual observations take the form of received power/range readings from the RADAR.

Section II briefly summarises related work, while section III describes how power-range spectra can be predicted. This utilises the RADAR range equation and a noise analysis which considers the propagation of noise from its source in the receiver through the RADAR electronics to the final range output. Methods for estimating the true range from power-range spectra are given in section IV where a new robust range estimation technique based on target presence probability is presented. Finally section V applies the analysis to a SLAM formulation based on MMW RADAR power-range spectra.

## II. Related Work

In recent years RADAR for automotive purposes has gained interest in shorter range $< 200$ metres applications. Most of the work in short range RADAR has focused on millimetre waves as this allows narrow beam shaping, which is necessary for higher angular resolution [1]. The work to date in autonomous navigation using millimetre wave RADAR is summarised here.

Clark [2] presented a method for fusing RADAR readings from different vehicle locations into a two-dimensional representation. The method selects one range point per RADAR power spectra observation at a particular bearing angle based on a certain threshold level. This method takes only one range reading per bin which is nearer to the RADAR, discarding all others. In [3] Clark shows a millimetre wave RADAR based navigation system which utilises artificial beacons for localisation and an extended Kalman filter for fusing multiple observations. Human assistance is required for adjusting the threshold as the returned signal power depends on all object's RCS.

Boehmke *et al.* [4] succeed in producing three-dimensional terrain maps using a pulsed RADAR with a narrow beam of $1^o$ and high sampling rate. The $1^o$ RADAR beam has a large antenna sweep volume and its large for robotic applications. Another design with a $2^o$ beam is has a reduced resolution. The efforts by Boehmke *et al.* shows the compromise between a narrow beam and antenna size, where a narrow beam provides better angular resolution.

Foessel shows the usefulness of evidence grids for integrating uncertain and noisy sensor information [5]. In [6], Foessel *et al.* show the development of a RADAR sensor model for certainty grids and also demonstrates the integration of RADAR observations for building three-dimensional outdoor maps. Certainty grids divide the area of interest into cells, where each cell stores a probabilistic estimate of its state [7] [8]. The proposed three-dimensional model by Foessel *et al.* has shortcomings such as the necessity of rigorous probabilistic formulation and difficulties in representing dependencies due to occlusion.

## III. RADAR Range Spectra Prediction

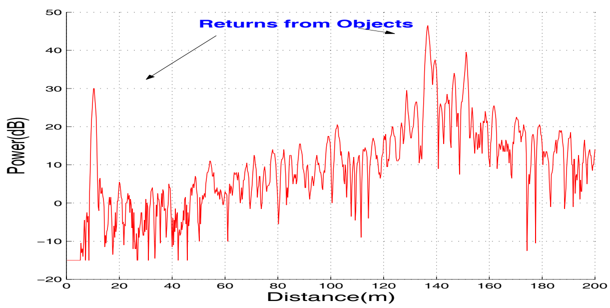


Fig. 1. RADAR Range Spectrum

Figure 1 shows a single RADAR range spectra, which is the received power versus range. As the RADAR signals can penetrate through most objects, we can achieve an entire range spectra at any particular bearing. The range bin, shown in figure 1 is obtained by keeping the RADAR pointed towards a RADAR corner reflector kept arbitrarily at 10.25 metres and the second dominant reflection occurs from a building which is 138 metres from the RADAR. *i.e.* the RADAR waves penetrates the corner reflector. The corner reflectors are of known RCS and can give good reflections back to the RADAR. The spectrum has two main features: the signal return from targets and noise. As shown in figure 1, signals are riding over a low frequency signal which increases its amplitude up to a certain range (150 metres approx.) and decreases towards the maximum range (200 metres approx.). This is due to the low pass filter roll-off in the RADAR receiver section.

A method for predicting the RADAR range spectra is now presented. The MMW RADAR range bin can be predicted from the RADAR range equation and from the knowledge of the received noise distribution. First, an introduction is given explaining the relation between RADAR signal return power and range. Next, a method for establishing the relationship between RCS and range of objects in outdoor environments is shown. A detailed noise analysis during signal absence and presence is then shown. This is necessary in predicting the range bins accurately during target presence and target absence. RADAR range bins are then predicted and the results are analysed.

### A. RADAR Range Equation

The RADAR returned power $P_r$ is proportional to the RADAR cross section of the object, $\sigma$ and inversely proportional to the fourth power of range, R [9]. The simple RADAR range equation is formally written as

$$P_r = \frac{P_t\, G^2\, \lambda^2\, \sigma}{(4\,\pi)^3\, R^4\, L} \tag{1}$$

where $P_t$ is the RADAR transmitted power; G is the Antenna Gain; $\lambda$ is the wavelength, (*i.e* 3.89 mm) and L the RADAR system losses. A high pass filter is used to compensate for the $R^4$ drop in received signal power. In an FMCW RADAR, closer objects correspond to signals with low beat frequencies and vice-versa. Therefore many RADARs incorporate signal processors which attenuate low frequencies and amplify high frequencies, to correct the range-based signal attenuation [10].

### B. RADAR Cross Section-Range Estimation

This section represents a method to establish the relative RADAR Cross Section (RCS) and range of objects in outdoor environments. RCS is a measure of the reflective strength of a RADAR target [11]. For a particular RADAR frequency, the RCS of an object is a function of geometric cross section of the object, reflectivity and directivity. Reflectivity is the ability of the target to reflect the RADAR signal which is not absorbed and directivity is the measure of energy returned to the RADAR [9].

The approach here is based on initially using reference targets with known RCS and finding out relative RCS of other objects by comparison. The objects in the environment are assumed to be point objects and the effect of side lobes of RADAR signals are currently ignored. Equation 1 can be represented using decibel-based units as

$$\begin{aligned} P_{r_{dBm}} = P_{t_{dBm}} \;+\; 2G_{dBi} + 20\log\lambda \;+\; 10\log\sigma \\ -\,30\log(4\,\pi) - 40\log R \;-\; L_{dB} \end{aligned} \tag{2}$$

where $P_{r_{dBm}}$ is the power received in dBm ; $P_{t_{dBm}}$ is the power transmitted in dBm; $G_{dBi}$ is the gain in dBi and RADAR losses in dB is represented as $L_{dB}$.

In equation 2, all terms are constant with the exception of object's RCS and range and atmospheric losses. The equation can be written as

$$P_{r_{dBm}} = K + 10\log\sigma - 40\log R \tag{3}$$

where $K$ represents all the RADAR parameters and atmospheric losses in dB; object range is R and its RCS is $\sigma$.

Experimental measurement of signal power, $P_{r_{dBm}}$ using an object with known RCS at a known range will give an estimate of the value of K. With the knowledge of K, we can then predict the *relative* RADAR cross section, $\hat{\sigma}$ based on the object range measurement, R and the returned power $P_{r_{dBm}}$.

The method explained here is useful in SLAM as we can predict the relative RCS of objects based on predicted observations which will allow feature discrimination so that features can be identified by parameters other than their coordinates.

## IV. Noise Reduction based on Target Presence Probability

To try and “pick-out” the true range values from range bins, previous methods have used a power threshold on the range bins (the first power to exceed some threshold gives the closest object) [2] or Constant False Alarm Rate techniques (CFAR) [12] [9]. The problem with the thresholding method is, it requires human interpretation/intervention for adjusting the threshold. The function of the CFAR processors is to maintain a constant and low rate of false alarms. A cell averaging (CA) detector is useful for maintaining a constant false alarm rate (CFAR) where the clutter power may be unknown and varying.

The CFAR method tends to work well with aircraft in the air having relatively large RCS, while surrounded by air (with extremely low RCS). At ground level however, the RCS of objects is comparatively low and also there will be clutter (objects which cannot be reliably extracted). The CFAR can then misclassify features as noise and noise as features. As the CFAR is a binary detection technique, the output is either a one or a zero; *i.e.* either target presence or target absence. The combination of subsequent observations is more difficult with this discrete representation. The problem arises when the technique classifies noise as signal. For typical outdoor environments, the RADAR cross section of objects may be small. The low returned power from these objects can be buried in noise. For extracting these lower signal returns, a method is now introduced which uses the probability of target presence [13] for feature detection. The detection problem described here can be stated formally as a binary hypothesis testing problem [14]. Feature detection can be achieved by estimating the noise power contained in the range spectra [15]. The noise estimate is performed by averaging past spectral power values and using a smoothing parameter. This smoothing parameter is adjusted by the target presence probability in the range bins. The target presence probability is obtained by taking the ratio between the local power of range spectra containing noise and its minimum. The noise power thus estimated is then subtracted from the range bins to give a reduced noise range spectra.

Let the signal-to-noise power, $\mathrm{P}_{SNP}(k,l) = \frac{\check{\mathrm{P}}(k,l)}{\mathrm{P}_{min}(k,l)}$ be the ratio between the local noisy power value and its derived minimum; where $\check{\mathrm{P}}(k,l)$ is the $k$-th power value of the $l$-th range spectra.

In the Neyman-Pearson test [16], the optimal decision (*i.e.* whether target is present or absent) is made by minimising the probability of the type II error, subject to a maximum probability of type I error is as follows.

The test, based on the *likelihood ratio*, is

$$\frac{p(\mathrm{P}_{SNP}\,|\,\mathrm{H}_1)}{p(\mathrm{P}_{SNP}\,|\,\mathrm{H}_0)} \underset{\mathrm{H}_0}{\overset{\mathrm{H}_1}{\gtrless}} \delta \tag{4}$$

where $\delta$ is a threshold; $\mathrm{H}_0$ and $\mathrm{H}_1$ designate hypothetical target absence and presence respectively. $p(\mathrm{P}_{SNP}\,|\,\mathrm{H}_0)$ and $p(\mathrm{P}_{SNP}\,|\,\mathrm{H}_1)$ are the conditional probability density functions. The decision rule of equation 4 can be expressed as

$$\mathrm{P}_{SNP}(k,l) \underset{\mathrm{H}_0}{\overset{\mathrm{H}_1}{\gtrless}} \delta \tag{5}$$

An indicator function, $\mathrm{I}(k,l)$ is defined where, $\mathrm{I}(k,l) = 1$ for $\mathrm{P}_{SNP} > \delta$ and $\mathrm{I}(k,l) = 0$ otherwise.

The estimate of the conditional target presence probability, $\hat{p}^{'}(k,l)$ is

$$\hat{p}^{'}(k,l) = \alpha_p \hat{p}^{'}(k,l-1) + (1-\alpha_p)\,\mathrm{I}(k,l) \tag{6}$$

This signal presence probability can be used as a target likelihood within the SLAM formulation. $\alpha_p (0 < \alpha_p < 1)$ is a smoothing parameter. The value of $\alpha$ is chosen in such a way that the probability of target presence in the previous range bin has very small correlation with the next range bin. The results of the proposed target detection algorithm are shown in figure 2 where a noisy RADAR range bin, the reduced noise range spectra and the corresponding target presence probability have been plotted. The probability of target presence vs. range of

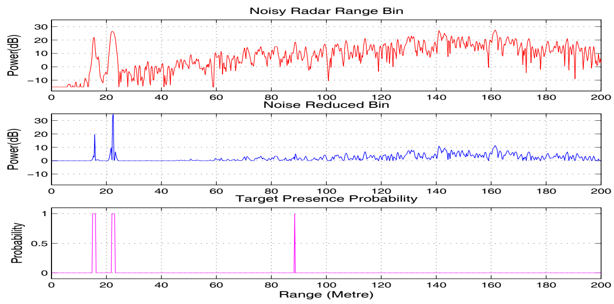


Fig. 2. Top graph: received range bin; Middle Graph: reduced noise graph; Lower Graph: probability of target presence versus range.

a two-dimensional RADAR scan obtained from an outdoor field is shown in figure 3. The features detected by the algorithm such as RADAR reflectors and a wall are marked in the figure. The probability of target presence is plotted against the vertical axis as shown in the figure. This representation of the environment provide a better correspondence with the actual environment compared with the other feature detections techniques such as applying a constant threshold on the power spectra and Constant False Alarm Rate (CFAR) techniques. In the constant threshold, operator assistance is required for adjusting the threshold for feature detection. CFAR techniques, due to the noisy range spectra, will produce false alarms. In cell-averaging CFAR, the averaging of cells provides a local estimation of the noise level. This locally estimated noise is used to define the threshold. The test window compares the threshold with the power of the signal and classifies the cell content as signal or noise. The CFAR method tries to detect object(s) in each observation.

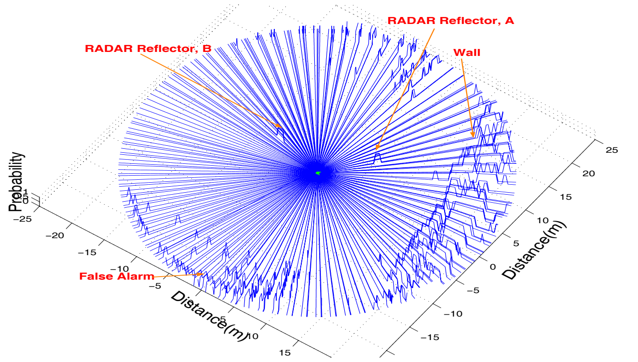


Fig. 3. Target presence probability vs. Range of a two-dimensional RADAR scan in outdoor environment. The scan is taken in a football field. The probability of the targets detected (*i.e.* RADAR reflectors A and B, and a wall) are shown in the figure.

When the signal and noise distribution has large separation in between, CFAR works well. But when the signal and noise distributions lie close together which is in this case, the method misclassifies noise as signal and vice versa. This is the reason for the poor performance of the CFAR technique with the noisy RADAR data.

As the RADAR signal can penetrate through most of the objects found in a natural environment, the range bin may have multiple peaks. The peaks lying close enough will adversely affect the estimation of noise. In these situations the threshold is set to high due to inaccurate noise estimation and this will lead to missed detection of features.

The proposed algorithm for feature extraction appears to outperform CFAR method because the CFAR method finds the noise locally while the target presence probability based feature detection estimates noise by considering more than one range bins

## V. Application: A Theoretically Correct SLAM Formulation using MMW RADAR

This section demonstrates an application of the RADAR analysis carried out so far. The analysis is used to correctly formulate a SLAM augmented state update formulation using MMW RADAR. The RADAR cross section, $\sigma$ and the RADAR loss constants, K are included in the state vector, along with the vehicle state and feature locations, as these variables are unique to a particular feature/RADAR. The SLAM formulation done here can handle *multiple line-of-sight features*.

### A. Simple Process Model

To illustrate the application, a very simple vehicle kinematic model is used for predicting the next vehicle location [17]. With reference to figure 4, the vehicle state, $\mathbf{x}_v(k)$ is given by $\mathbf{x}_v(k) = [x(k), y(k), \theta(k)]^T$ where $x(k)$, $y(k)$ and $\theta(k)$ are the local position and orientation of the vehicle at time $k$. The vehicle state, $\mathbf{x}_v(k)$ is propagated to time $(k+1)$ through a process model. The model with control inputs, $\mathbf{u}(k)$ to the vehicle; predicts the vehicle state at time $(k+1)$ together with the uncertainty in vehicle location represented in the covariance matrix $\mathbf{P}(k+1)$.

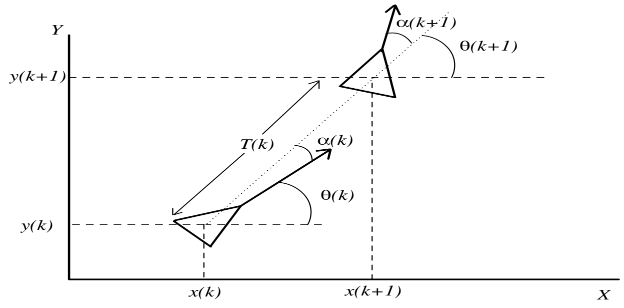


Fig. 4. Vehicle model. $T(k)$ is the distance traveled by the vehicle from time $k$ to $k+1$ and $\alpha(k)$ is the steer angle.

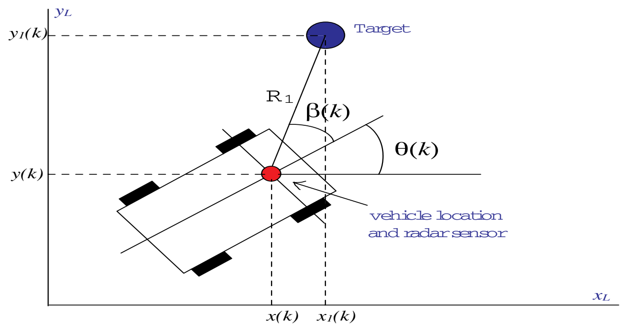


Fig. 5. Vehicle coordinate system and beacon observation

$$\mathbf{x}_v(k+1) \quad = \quad \mathbf{f}\left(\mathbf{x}_v(k)\,,\,\mathbf{u}(k)\right) + \mathbf{v}(k) \tag{7}$$

where $\mathbf{u}(k)$ is the control input to the vehicle; $\mathbf{u}(k) = [T(k)\,,\,\alpha(k)]$. $T(k)$ is the distance traveled by the vehicle from time $k$ to $k+1$ and $\alpha(k)$ is the rotation angle. In full, the predicted state at time, $k+1$ becomes

$$\begin{bmatrix} \hat{x}(k+1\,|\,k) \\ \hat{y}(k+1\,|\,k) \\ \hat{\theta}(k+1\,|\,k) \\ \mathrm{x}_{p_1}(k+1\,|\,k) \\ \mathrm{y}_{p_1}(k+1\,|\,k) \\ \sigma_{p_1}(k+1\,|\,k) \\ \vdots \\ \mathrm{x}_{p_N}(k+1\,|\,k) \\ \mathrm{y}_{p_N}(k+1\,|\,k) \\ \sigma_{p_N}(k+1\,|\,k) \\ \mathrm{K}(k+1\,|\,k) \end{bmatrix} = \begin{bmatrix} \hat{x}(k\,|\,k) \\ \hat{y}(k\,|\,k) \\ \hat{\theta}(k\,|\,k) \\ \mathrm{x}_{p_1}(k\,|\,k) \\ \mathrm{y}_{p_1}(k\,|\,k) \\ \sigma_{p_1}(k\,|\,k) \\ \vdots \\ \mathrm{x}_{p_N}(k\,|\,k) \\ \mathrm{y}_{p_N}(k\,|\,k) \\ \sigma_{p_N}(k\,|\,k) \\ \mathrm{K}(k\,|\,k) \end{bmatrix} + \begin{bmatrix} T(k)\cos(\hat{\theta}(k\,|\,k) + \alpha(k)) \\ T(k)\sin(\hat{\theta}(k\,|\,k) + \alpha(k)) \\ \alpha(k) \\ 0_{p_1} \\ 0_{p_1} \\ 0_{p_1} \\ \vdots \\ 0_{p_N} \\ 0_{p_N} \\ 0_{p_N} \\ 0 \end{bmatrix} \tag{8}$$

The augmented state vector is then $\mathbf{x}(k) = [\mathbf{x}_v, \{\mathbf{F}_1, \sigma_{p_1}\} \dots \{\mathbf{F}_i, \sigma_{p_i}\}, \dots \{\mathbf{F}_N, \sigma_{p_N}\}, K]^T$; $\mathbf{x}_v$ is the vehicle pose; $\mathbf{F}_i = [\mathrm{x}_{p_i}, \mathrm{y}_{p_i}]^T$ is the $i$-th feature location, where $1 \leq i \leq N$. $\sigma_{p_i}$ is the relative RADAR cross section of the $i$-th feature and $K$ is the RADAR specifications together with losses which can be calculated as shown in the previous section. $\mathbf{v}(k) = [\mathbf{v}_v(k), 0_{p_1}, 0_{p_1}, \mathrm{v}_{\sigma_1}, \dots, 0_{p_i}, 0_{p_i}, \mathrm{v}_{\sigma_i}, \dots, 0_{p_N}, 0_{p_N}, \mathrm{v}_{\sigma_N}, 0]^T$. The SLAM considers that all features are stationary but the RCS of features changes from different angles compared to the RADAR locations and can be modeled using a Gaussian random variable, $\mathrm{v}_{\sigma_i}$.

### B. Observation Model

The RADAR observation is used to estimate the vehicle state once the vehicle pose is predicted. During filter update, the prediction and estimation are fused. For each of the features in the map, the range, $R(k+1\,|\,k)$, the RADAR bearing angle, $\beta(k+1\,|\,k)$ and the power, $\breve{\mathrm{P}}(k+1\,|\,k)$ are predicted from the predicted vehicle location in equation (8).

$$R_i(k+1) = \sqrt{[x_{p_i}(k+1) - x(k+1)]^2 + [y_{p_i}(k+1) - y(k+1)]^2} + v_R(k+1) \tag{9}$$

$$\beta_i(k+1) = \tan^{-1}\left[\frac{y_{p_i}(k+1) - y(k+1)}{x_{p_i}(k+1) - x(k+1)}\right] - \theta(k+1) + v_\beta(k+1) \tag{10}$$

$$\mathrm{P}_i(k+1) = K + 10\log\sigma_{p_i}(k+1) - 40\log R_i(k+1) + v_P(k+1) \tag{11}$$

where $v_R(k) \sim N(0, \sigma_R{}^2)$, $v_\beta(k) \sim N(0, \sigma_\beta{}^2)$, and $v_P(k) \sim N(0, \sigma_P{}^2)$. Equations 9, 10 and 11 between them comprise the observation. The error in range, and power, $v_P(k)$ is experimentally obtained [13]. The angular standard deviation is assumed to be $1^o$ as the RADAR wave is a pencil beam. The observation model is then given by

$$\begin{aligned} \mathbf{z}_i(k+1) &= [\mathrm{R}_i(k+1), \beta_i(k+1), \mathrm{P}_i(k+1)]^T \\ &\quad + \mathbf{w}_i(k+1) \\ &= \mathbf{h}(\mathbf{x}(k+1)) + \mathbf{w}_i(k+1) \end{aligned} \tag{12}$$

where $\mathbf{z}_i(k+1)$ is the observation, and $\mathbf{w}_i(k+1)$ is the additive observation noise. ($\mathbf{w}_i(k+1) = [v_R(k+1)\; v_\beta(k+1)\; v_p(k+1)]^T$) and $\mathbf{h}$ is the non-linear observation function.

### C. Results

Implementation and integration of the vehicle and target state predictions together with the RADAR predicted and true observations can then continue under the usual EKF, UKF or particle filter algorithms. To highlight the contributions of this paper, the initial stages of a SLAM implementation will be shown in terms of predicting, measuring and gating RADAR range bins. The RADAR was mounted on a utility vehicle (figure 6) and measurements were obtained from an outdoor field. A single range spectra at the starting location is as shown in figure 7. All range bins from a full 360 scan are now collected, and predicted targets are extracted. The next predicted vehicle location is calculated using the vehicle model and system inputs. The range spectra in all directions are then predicted from the new predicted vehicle location. From the actual new

Fig. 6. Test vehicle with MMW RADAR and GPS

vehicle position, new range bins are recorded. These are compared with the predicted range bins in figures 8 and 9.

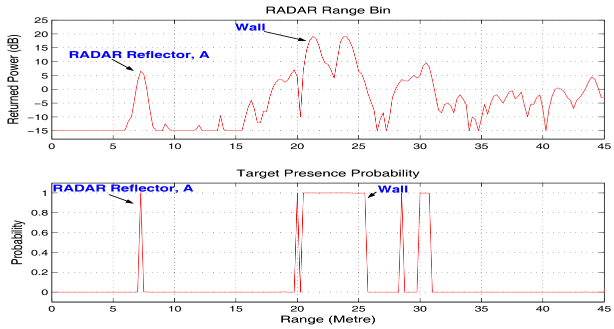


Fig. 7. Range spectra obtained from the starting vehicle location and the corresponding target presence probability.

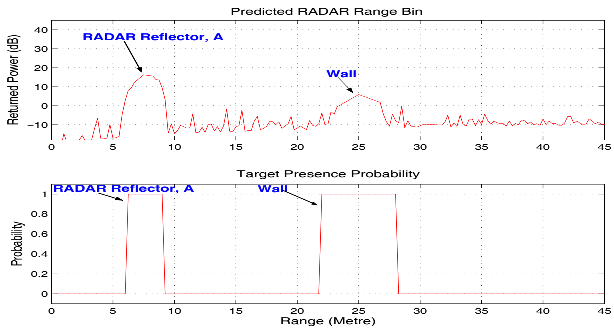


Fig. 8. Predicted range spectra from the predicted vehicle location and the corresponding predicted target presence probability.

In figure 8 the predicted range bins are shown. For the RADAR data received at time, $k+1$, from bearing angles $\beta_1'$ and $\beta_2'$ (defined in figure 10), the predicted target spikes are clearly visible.

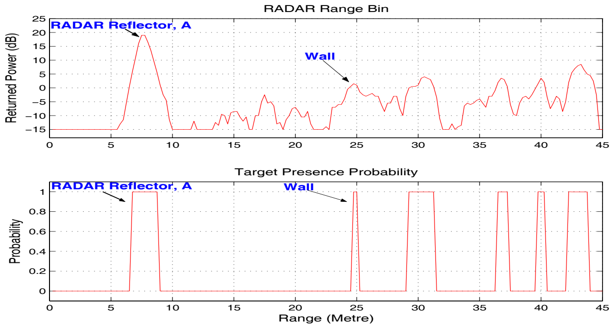


Fig. 9. Actual range spectra obtained from the next vehicle location and the corresponding target presence probability.

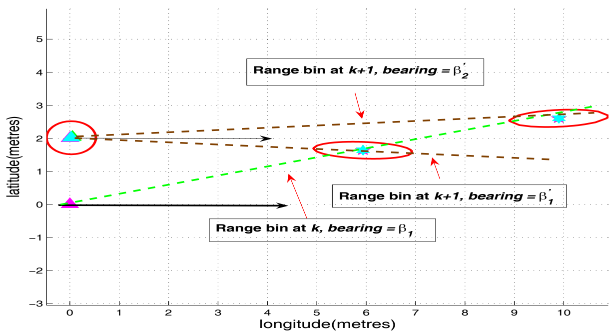


Fig. 10. SLAM Formulation - Predicted and actual measurements.

In figure 9 the actual range bins are shown for the corresponding bearing angles, recorded from the vehicles true position at time, $k+1$.

The predicted range bin considers only two objects down-range. When the radar is "looking straight" on a flat surface (eg. wall), the RADAR return signal will be narrow compared to when the RADAR viewing the same object at some angle [6]. The real RADAR spectra shown in figure 9 contains multiple features which results in more peaks in the corresponding target presence probability plot. The range spectra prediction explained in this paper does not consider the antenna beam width and the grazing angle with which the RADAR beam falls on the target. This will be addressed in the future work. Figure 10 shows the predicted targets and their $3\sigma$ error covariance ellipsi and the measured targets. The "initialisation" of a SLAM process shows the ability of gating multiple line-of-sight features, an ability unique to RADAR.

## VI. Conclusion

The paper shows a method for estimating the relative RADAR cross section of objects. This is useful in SLAM as we can predict the relative RCS of objects based on predicted observations which will allow feature discrimination so that features can be identified by parameters other than their coordinates. A new augmented state vector for an Extended Kalman Filter is introduced which includes relative RADAR cross sections of features, and the RADAR constants and losses along with the vehicle pose and feature locations. An estimate of the received noise when a target is present and in target absence has been carried out for accurately predicting the RADAR power-range spectra. The initialisation of a SLAM formulation using the proposed methods was shown. This work is a step towards building reliable maps and localising a vehicle to be used in mobile robot navigation. In the future work, quantifying the bearing angle errors will be addressed. A more accurate method for range spectra prediction, which considers the antenna beam width, will also be implemented. Inclusion of absorbtion coefficient of RADAR signals by the features to the state matrix will be investigated. This will be helpful in dealing with multiple targets down range.

## VII. Acknowledgements

This work was funded under the second author's AcRF Grant, RG 10/01, Singapore. We gratefully acknowledge help from SIMTech in the use of their utility vehicle and valuable advice from Graham Brooker (ACFR) and Steve Clark (Navtech Electronics, UK).

## References

[1] Graham Brooker, Mark Bishop, and Steve Scheding. Millimetre waves for robotics. In *Australian Conference for Robotics and Automation*, Sidney, Australia., November 2001.

[2] Steve Clark. *Autonomous Land Vehicle Navigation Using Millimetre Wave Radar*. PhD thesis, Australian Centre for Field Robotics, University of Sydney, 1999.

[3] Steve Clark and Hugh Durrant-Whyte. Autonomous land vehicle navigation using millimeter wave radar. In *ICRA*, pages 3697–3702, 1998.

[4] Scott Boehmke, John Bares, Edward Mutschler, and Keith Lay. A high speed 3d radar scanner for automation. In *Proceedings of ICRA '98*, volume 4, pages 2777–2782, May 1998.

[5] Alex Foessel. *Scene Modeling from Motion-Free Radar Sensing*. PhD thesis, Robotics Institute, Carnegie Mellon University, Pittsburgh, PA, January 2002.

[6] Alex Foessel, John Bares, and William Red L. Whittaker. Three-dimensional map building with mmw radar. In *Proceedings of the 3rd International Conference on Field and Service Robotics*, Helsinki, Finland, June 2001. Yleisjljenns - Painnoprssi.

[7] Hans Moravec and A. E. Elfes. High resolution maps from wide angle sonar. In *Proceedings of the 1985 IEEE International Conference on Robotics and Automation*, pages 116–121, March 1985.

[8] Sebastian Thrun. Learning occupancy grids with forward models. In *Proceedings of the Conference on Intelligent Robots and Systems*, Hawaii, 2001.

[9] M.I Scolnik. *Introduction to Radar Systems*. McGraw Hill, New York, 1982.

[10] Dirk Langer. *An Integrated MMW Radar System for Outdoor Navigation*. PhD thesis, Robotics Institute, Carnegie Mellon University, Pittsburgh, PA, January 1997.

[11] D. Barton and S. Leonov. *Radar Technology Encyclopedia*. Artech House, Norwood, 1997.

[12] N.C Currie and C.E.Brown. *Principles and Applications of MMW Radar*. Artech House, Dedham,MA, 1987.

[13] Ebi Jose and Martin D. Adams. Millimetre wave radar spectra simulation and interpretation for outdoor slam. In *International Conference on Robotics and Automation*, New Orleans, USA, April 2004.

[14] H.L. Van Trees. *Detection, Estimation and Modulation Theory - Part I*. Willey, New York, 1968.

[15] Israel Cohen and Baruch Berdugo. Noise estimation by minima controlled recursive averaging for robust speech enhancement. In *IEEE Signal Processing Letters*, volume 9, 2002.

[16] T. Kirubarajan and Y.Bar-Shalom. *Multisensor-Multitarget Statistics in Data Fusion Handbook*. CRC Press,Boca Raton, 2001.

[17] Jeffrey K. Uhlmann. *Dynamic Map Building and Localization: New Theorecital Foundations*. PhD thesis, Robotics Research Group, Department of Engineering Science, University of Oxford, 1995.